AMEGHINIANA
A GONDWANAN PALEONTOLOGICAL JOURNAL

Submitted: May 6th, 2015 – **Accepted**: August 28th, 2015

To link and cite this article:

doi: 10.5710/AMGH.24.08.2015.2917

TAPHONOMIC ANALYSIS AND PALEOBIOLOGICAL OBSERVATIONS OF *CROSSVALLIA UNIENWILLIA* TAMBUSSI *ET AL.* 2005, THE OLDEST PENGUIN FROM ANTARCTICA

ANÁLISIS TAFONÓMICO Y OBSERVACIONES PALEOBIOLÓGICAS DE *CROSSVALLIA UNIENWILLIA* TAMBUSSI *ET AL*. 2005, EL PINGÜINO MÁS ANTIGUO DE ANTÁRTIDA

CAROLINA ACOSTA HOSPITALECHE[1,4], LEANDRO M. PÉREZ[2,4], SERGIO MARENSSI[3] AND MARCELO REGUERO[1,4]

[1].- División Paleontología de Vertebrados, Museo de La Plata, Facultad de Ciencias Naturales y Museo (UNLP). Paseo del Bosque, La Plata B1900FWA, Argentina. acostacaro@fcnym.unlp.edu.ar, regui@fcnym.unlp.edu.ar,

[2].- División Paleozoología de Invertebrados, Museo de La Plata, Facultad de Ciencias Naturales y Museo (UNLP). Paseo del Bosque, La Plata B1900FWA, Argentina. pilosaperez@gmail.com

[3].- IGeBA (Universidad de Buenos Aires – CONICET). Dto. Ciencias Geológicas – FCEyN. Ciudad Universitaria-Pabellón 2, 1° piso. Buenos Aires C1428EHA, Argentina. smarenssi@hotmail.com

[4].- CONICET.

33 pag. (text+references); 6 fig.

Abstract. The purpose of the present paper is the taphonomic analysis of the holotype of *Crossvallia unienwillia* Tambussi, Reguero, Marenssi and Santillana, 2005 in order to improve the knowledge of the vertebrate record of the Cross Valley Formation, cropping out at the central area of Marambio (Seymour) Island, Antarctic Peninsula. The analyses of the preservational state of the skeleton assigned to *Crossvallia unienwillia* offer important data for palaeonvironmental and depositional reconstructions, key for the understanding of the early evolutionary history of penguins. Different techniques, including petrographic sections, observation in SEM, secondary Electrons detectors, backscattered electrons detectors, microanalysis for probe of electrons, and X-ray diffraction were applied in order to distinguish biostratinomic from fossil diagenetic damage. Fossil bones of *Crossvallia* are associated with a typical marine assemblage including shark remains and macroinvertebrates. The hosting mudstones point to a low-energy environment either below the wave-base or protected from the wave action. In any case initial marine conditions changed to other with regular influx of land-derived sedimentary material. *Crossvallia unienwillia* was a female diver that passed through several molting periods before death. Biostratinomic processes consistent with little transport and rapid burial which would have prevented the action of destructive processes such as weathering and carnivores or scavenging, are inferred. The rapid burial favored the initial preservation of the elements under anoxic conditions. The surficial corrosion, fractures, and the internal filling of the cavities, suggest that destructive processes were only important after final burial during the telodiagenetic stage. The absence of more vertebrate fossil remains in the *Cross Valley C* Allomember is the result of those destructive processes, whereas on the contrary the original depositional environment appears to be optimal.

Key words. Fossil Penguin, Cross Valley, Marambio Island, Paleocene, Antarctic Peninsula.

Resumen. ANÁLISIS TAFONÓMICO DE *CROSSVALLIA UNIENWILLIA* TAMBUSSI *ET AL*. 2005: EL PINGÜINO MÁS ANTIGUO DE ANTARTIDA. El objetivo del presente trabajo es el análisis tafonómico del holotipo de *Crossvallia unienwillia* Tambussi, Reguero, Marenssi and Santillana, 2005, con el fin de incrementar el conocimiento acerca del registro fósil de vertebrados de la Formación Cross Valley, aflorante en el área central de la Isla Marambio (Seymour), Península Antártica. El análisis del estado preservacional de los restos de *Crossvallia unienwillia* ofrece importantes datos para las reconstrucciones paleoambientales y áreas depositacionales, claves para la comprensión de la historia evolutiva temprana de los pingüinos. Diferentes técnicas, incluyendo el estudio de secciones petrográficas, observaciones en MEB, detector de electrones secundarios, detector de electrones dispersos, difracción de rayos X y rayos X de energía dispersiva, fueron aplicados para distinguir las alteraciones bioestratinómicas de aquellas fósil-diagenéticas. Los restos de *Crossvallia* forman parte de una asociación típicamente marina, incluyendo además tiburones y macroinvertebrados. Los sedimentos portadores indican un ambiente de baja energía, ya sea por debajo del tren de olas, o bien protegido de la acción de las olas. En cualquiera de estos casos, las condiciones marinas iniciales cambiaron hacia otras con un flujo regular de material continental sedimentario. *Crossvallia unienwillia* fue una hembra buceadora, que atravesó varios periodos de muda antes de su muerte. Procesos bioestratinómicos consistentes con un bajo transporte y un rápido sepultamiento que habría prevenido la acción de procesos destructivos tales como la meteorización son inferidos para este caso. El enterramiento rápido favoreció la preservación de los elementos bajo

condiciones anóxicas. La corrosión superficial, las fracturas y el relleno de cavidades internas, sugiere que los procesos destructivos fueron solo importantes luego del sepultamiento durante estadios telodiagenéticos. La ausencia de otros vertebrados fósiles en el Alomiembro *Cross Valley C* es el resultado de esos procesos, mientras que de manera contraria, el ambiente depositacional pareció haber sido óptimo.

Palabras clave. Pingüino fósil, Cross Valley, Isla Marambio, Paleoceno, Península Antártica.

THE material for this study comes from the type section of the Late Paleocene Cross Valley Formation (Elliot and Trautman, 1982; Montes *et al*., 2013) located at the central area of Marambio (Seymour) Island, Antarctic Peninsula. The Cross Valley Formation is limited by two main unconformities from the underlying Danian Sobral Formation (and probably also from the Maastrichtian-Danian López de Bertodano Formation) and the overlying Eocene La Meseta Formation (Santillana and Marenssi, 1997; Montes *et al*., 2007; Marenssi *et al*., 2012) respectively. Dinoflagelates and Strontium-derived ages (Sr^{87}/Sr^{86}) allowed estimating a Selandian-Thanetian age for this unit (Palamarczuk *et al*., 1984; Askin, 1988; Wrenn and Hart, 1988; Marenssi and Santillana, 2003).

Among vertebrates, which are scarce in this unit, non-articulated partial penguin skeleton assigned to *Crossvallia unienwillia* Tambussi, Reguero, Marenssi and Santillana, 2005, an isolated penguin diaphysis and some fish bones were recovered. The penguin diaphysis (MLP 00-I-1-16) belongs to a Spheniscidae indet., consistent in size with *Crossvallia unienwillia* but badly preserved. Fish material includes several bony fragments of Teleostei *indet*. (MLP 00-I-17 and MLP 00-I-18) and shark teeth (MLP 14-I-10-82). Holotype of *Crossvallia unienwillia* is the only skeleton known for this unit (MLP 00-I-10-1); fossils were found associated and constitute the holotype and only elements known for this species (Tambussi *et al*., 2005; Jadwiszczak *et al*., 2013a).

Successive paleontological field work in this locality corroborated the scarcity of vertebrates of this unit. By contrast, fossil leaves and other plant remains are common in the upper part of the same level (Dusén, 1908; Cantrill *et al*., 2011). *Crossvallia* represents an important case, not only for the study of penguins and the Antarctic fauna in general, but because it helps understanding the taphonomic history of the vertebrates from the Cross Valley Formation.

105 The analyses of the preservational state of *Crossvallia unienwillia* offer important
106 data for palaeonvironmental and depositional reconstructions, and constitute a key for the
107 understanding of the evolutionary early history of penguins. This knowledge may result
108 extremely useful for planning and prospecting these strata in the near future. In this sense,
109 the purpose of the present paper is the taphonomic analysis of the fossil remains, either
110 biostratinomic or fossil diagenetic, to improve the knowledge of the vertebrate fossil record
111 in the Cross Valley Formation.
112
113 **GEOLOGIC SETTING**
114 The Cross Valley Formation is 195 meters thick and fills in a narrow valley with
115 volcaniclastic deposits representing an incised valley system, including estuarine, shallow
116 marine and deltaic facies (Marenssi *et al*., 2012). Recent field work allowed to subdivide
117 this formation into three unconformity bounded subunits or allomembers named A to C
118 from base to top (Santillana *et al*., 2007; Marenssi *et al*., 2012; Montes *et al*., 2013). A
119 detailed sedimentological and petrographic description of this unit has been recently
120 presented by Marenssi *et al*. (2012).
121
122 *Cross Valley A Allomember*: The base of the unit is a 0.30 to 1 meter thick medium-grained
123 massive sandstone bed rich in glaucony. The bulk of the allomember is composed of
124 coarse- to fine-grained cross-bedded sandstones with a high percentage of volcanic material
125 arranged into three fining upward cycles 30 to 40 meters thick. Charred wood is frequently
126 found in the sandstones. This allomember is interpreted as deposited in subtidal channels
127 within an incised valley (Montes *et al*., 2007; Marenssi *et al*., 2012).

Cross Valley B Allomember: The base of this unit is a subtle erosive surface mantled by coarse-grained to gravely sandstones. Three main lithofacies of about 35 m thickness compose this allomember. A lower interval made up of coarse-grained massive sandstones, a middle part composed of coarse- to medium-grained parallel-laminated sandstones and an upper section made up of interbedded medium-grained sandstones and mudstones. Angular to subangular volcanic clasts, including pumice, comprise more than 80 % of the sand and gravel fraction. This allomember records submarine volcaniclastic (laharic-type?) sedimentation within an incised valley (Amoedo, 1992; Doktor *et al*., 1988; Montes *et al*., 2007; Marenssi *et al*., 2012).

Cross Valley C Allomember: This unit of about 15-20 m thickness, covers the former by means of an erosive surface locally draped by angular blocks (up to 0.40 m in diameter) of the underlying unit. The lower part is composed of gray calcareous mudstones containing occasional fish and shark teeth, gastropods, echinoids and penguin bones (Tambussi *et al*., 2005). The upper part is made up of interbedded fine-grained parallel-laminated to ripple cross-laminated light sandstones and dark mudstones containing large wood fragments and discrete levels of plant debris (Dusén, 1908; Cantrill *et al*., 2011). The sandstone composition changes from base to top. Rock fragments in the sand-sized fraction are dominated by volcanics in the base but plutonic and metamorphic detritus become dominant towards the top. Sandstones are mainly cemented by calcium carbonate (both sparite and micrite) but some diagenetic clays and iron oxides are locally present. This allomember represents sedimentation in shallow marine to marginal deltaic (interdistributary bays) environments (Elliot and Trautman, 1982; Marenssi *et al*., 2012).

The Cross Valley Formation has been interpreted as representing different sedimentary environments within a coastal setting. Elliot *et al*. (1975) interpreted

sedimentation in mixed fluvial and deltaic environments, while later Elliot and Trautman (1982) restricted their interpretation to a deltaic origin. Later, Sadler (1988) demonstrated that the Cross Valley Formation fills in a narrow submarine valley. Doktor *et al*. (1988) and Amoedo (1992) described deltaic and volcaniclastic lahar-like deposits. Finally, Montes *et al*. (2007) and Marenssi *et al*. (2012) interpreted the Cross Valley Formation as an incised valley fill system with a lower subtidal volcaniclastic section (allomembers A and B) and an upper deltaic member (Allomember C).

MATERIALS AND METHODS

Materials under study are housed in the Museo de La Plata (MLP), La Plata, Argentina. The penguin fossil bones (MLP 00-I-10-1 and MLP 00-I-1-16), and the fish remains (MLP 00-I-17, MLP 00-I-18, and MLP 14-I-10-82) were collected during field works organized by the Instituto Antártico Argentino, in the Late Paleocene Cross Valley Formation (lower part of Allomember C) at the locality GPS: 64° 15′ 50′′ S, 56° 40′ 0′′ W (Fig. 1.1) (Seymour-Marambio Island), Antarctica (see Tambussi *et al*., 2005).

Penguin material was described using a stereoscopic microscope Arcano ZTX Zoom (10-40x). Fractures were classified according to their genesis, distinguishing biostratinomic from fossil diagenetic damage following the classical criteria of Behrensmeyer (1978).

Osteological terminology follows Baumel and Witmer (1993), and measurements were taken with a Vernier Caliper with an accuracy of 0.1 mm. The ratio of the marrow area to the whole section of the bone was calculated following Meister (1962).

The petrographic analysis was made on a thin section of long bone prepared by the total rock technique. A binocular microscope Zeiss STEMI 2000-C with a camera CANON

power Shot C10 was used for obtaining a general image of the CT. The thin sections were analyzed with a petrographic microscope Leitz Laborlux 12 Pol with a photographic digital camera Leica DFC290 HD. Images were captured through the Leica Application Suite V3 version 3.7; pictures were taken with plane-polarizer (pp) and without plane-polarizer (wp).

For the observation of the material in SEM (Scanning Electron Microscope), model FEI ESEM Quanta 200 with electron source from a tungsten filament, with accelerating voltage of 200 V – 30 kV from the Departamento de Mecánica, service LIMF (Facultad de Ingeniería, UNLP) was used. The sample was analyzed in Low Vacuum mode (LoVac) with a precision of 0.1 to 1 Torr, without metalizing. Secondary Electrons detectors, were used looking for a high topographic contrast image of the examined surface.

Backscattered electrons (BE) detectors of two sectors BSED were employed in order to observe variations in the atomic number (Z) of the elements detected on surface. Heterogeneity of the sample is expressed in the image through different gray tonalities regarding the atomic number (a further explanation can be consulted in Galván Josa *et al*., 2013).

Microanalysis for probe of electrons (dispersive in energy X-ray Spectrometer) EDAX SDD Apollo 40 was performed. It implies the detection of light elements from boron, resolution <135 eV, with a qualitative, semi-quantitative, and quantitative analysis capacity, and patterns for chemical elements microanalysis in a sample of 1 mm^3.

The X-ray diffraction analysis was made on a fine material sifted by a mesh (<20 microns), measured with a PANalytical X´Pert PRO diffractometer with a CU lamp (k=1.5403 Å), to 40 m Å and 40 kV. Samples were measured from 4 to 37°, with a scanning speed of 0.04°/s. The software Origin was selected for the edition of the results. This study and the petrographic analysis were made in the Centro de Investigaciones

Geológicas (CIG – CONICET) from La Plata. Samples were represented by bony fragments associated to the holotype of *Crossvallia unienwillia*, the Spheniscidae indet. from the Late Eocene Submeseta Formation, and the living *Pygoscelis adeliae* (Hombron and Jacquinot, 1841).

Stratigraphy is according to Marenssi *et al*. (2012) and Montes *et al*. (2013).

RESULTS

Crossvallia unienwillia (holotype MLP 00-I-10-1) was described on the basis of a partial skeleton (almost complete left humerus and right femur, proximal and distal end of right tibiotarsus, an incomplete thoracic vertebra and other 28 unidentifiable remains, see Jadwiszczak et al., 2013a), whose elements were found associated on surface (Fig. 2).

Macroscopic observations

The *humerus* is complete but preserved in several pieces. The periostial bone layer and both epiphyses are well preserved, but some signs of chemical alteration, such as the change in the composition of the surficial bone, are observed. Quartz grains are accreted at the proximal end, and other siliciclastic sediments are added in patches on the diaphysis. The tridimensional relationships are well preserved with no observable deformation. Signs of surface weathering (according to Behrensmeyer, 1978) or flaking off in the periosteal bone are absent. Neither longitudinal fractures along the main axis nor any fracture with eyelet morphologies are present. On the contrary, perpendicular or oblique fractures are abundant in the diaphysis (Fig. 3.1). The internal cavity is not filled or substituted by sediment, and trabecular tissues are observed.

The *femur* is badly damaged, and preserved in several pieces. The periostial bone layer and the epiphyses are highly altered by chemical corrosion (Fig. 3.2). Osteological

224 features at the proximal end are abraded and covered by sulfate deposits. Signs of
225 weathering are mainly observed at the distal end, leaving uncovered the trabecular bone. By
226 contrast, the diaphyseal periosteal bone remains non-flaked, and mineral precipitates fill the
227 inner spaces of the shaft.

228 The epiphyses of the *tibiotarsus* (and a little portion of the diaphysis) are completely
229 damaged and present transversal fractures (Fig. 3.3). The same preservational attributes
230 described for the proximal end of the femur (Fig. 3.2) are present here (mineral deposits,
231 corrosion, etc).

232 The unidentified fragments associated with the holotype of *Crossvallia* have flat and
233 clean fractures, perpendicular to the bony tissue fibers. The characteristic
234 pachyosteosclerosis developed in all penguin bones is also present here. However, the
235 degree of specialization is lower than that of recent penguins (see discussion below).

236 In summary, signs of weathering such as longitudinal fractures, flaking and polishes
237 surface are not observed in these bones. Traces attributed to trampling by other animals,
238 scavenging or carnivores marks (Cione *et al.*, 2010) were neither identified.

239

240 ***Microscopic observations (Petrographic section)***

241 *Histology*.- The histological arrangement of the bone in the specimen of *Crossvallia*
242 *unienwillia* is similar to other birds (Meister, 1951), with only differences in the
243 distribution of the bony fabric. The concentric histological structure previously recognized
244 in modern penguins (Meister, 1962; de Margerie *et al*., 2004) and also in extinct forms
245 (Yury-Yáñez *et al*., 2012; Cerda *et al*., 2015) is here observed (Fig. 4.1). It includes the
246 development of pachyosteosclerosis (Houssaye, 2009) according to the classification of de

247 Ricqlès and de Buffrénil (2001) for bone hypertrophy non- associated to pathological
248 contexts.

249 A detailed comparison of the proportions of each bony layer in the different penguin
250 species allows the recognition of different levels or degrees of specializations (see below).
251 In *Crossvallia*, the periosteal bone is moderate, the compact bone represents the main part
252 of the volume, and the trabecular bone constitutes an intermediate layer in volume
253 contacting and invading the marrow cavity (Fig. 4.2). The relationship between the
254 medullar cavity and the wall thickness is 1: 2.03 in the specimen of *Crossvallia unienwillia*
255 (see Meister, 1962), meaning that the medullar area occupies about the 49% of the area in
256 section.

257 The periosteal bone layer is the dark brownish layer composed by an outer dense
258 fibrolamellar tissue with few vestigial vascular spaces and canaliculi (Fig. 4.3). It
259 constitutes the 8% of the ratio in the transversal section.

260 Toward the inner part, two compact bone areas equal in size form 51% of the ratio.
261 The most external one is compact and less vascularized, with a denser bioapatite matrix.
262 The inner one is characterized by a more vascularized tissue (Fig. 4.2, 4.5). Abundant and
263 well defined primary osteons with Haversian system surrounded by lamellae and canaliculi
264 are homogeneously distributed. They constitute large cavities originated by resorption that
265 sometimes are partially filled by carbonates with centrifugal growing and other amorphous
266 compounds (Fig. 4.5 and 4.6). Vascular spaces and Volkmann´s canals extend from the
267 marrow area to the periosteal bone (Fig. 4.6). Remnants of destroyed Haversian system
268 appear in Fig. 4.5.

269 Trabecular bone occupies the 13% of the ratio and constitutes two different zones.
270 A light layer (Fig. 4.2) between the inner compact bone and the medullar bone with few

Volkmann canals (Fig. 4.4), and a most internal marrow area partially invaded by medullar bone. Secondary osteons are surrounded by lamellar tissue (Fig. 4.5). Frequent cavities (sometimes curved) formed by the enlargement of the Volkmann canals present mineral deposits with centrifugal growing (Fig. 4.6).

Preservational state.- In the image analyzed without plane-polarizer (Fig. 4.2, 4.3), a series of fractures can be distinguished. The most conspicuous (Fig. 4.2) is located at the left lower corner, showing a diaclase morphology (F1) and runs across the complete section of the bone reaching the marrow space (Fig. 4.1). This central space is partially filled by carbonates with fibrous or granular textures (Fig. 4.5, 4.6). Radial fractures observed in the left upper corner (Fig. 4.2) cut across the compact periosteal bone layer, reaching the most peripheral cancellous bone, where it changes the direction becoming tangential to the concentric layers (F2). A set of fractures of minor development starts from F2 (in the periosteal bone layer), taking an opposite direction. In the external portion of the bone, a very compact fraction of periosteal bone (Pb) can be distinguished. It is damaged by corrosion, with peeling signs on its external part, and fractures subparallel (F3) to the layers of the fibrolamellar tissue (Ft) filled by mineral compounds, (Fig. 4.3).

The middle part of the bone (Fig. 4.2) is represented by external compact bone (Ecb) with a few narrow canaliculi (c), some of them filled by mineral compounds (Cc). On the contrary (Fig. 4.5), the inner compact bone (Icb), is crossed by many thick canaliculi which are completely filled by carbonatic cement (Cc). The deepest osteological tissue (Fig. 4.5), identified as trabecular compact bone (Tb), leaves wide empty spaces completely obliterated by mineral cement (Cc). Under polarized light, the same image allows identifying the fibers organization (Fig. 4.4, 4.6) showing the highest density of the external portion of compact bone (Fig. 4.4), and the highest porosity of the inner compact bone (Fig.

295 4.6). Also, the high birefringence of the carbonate cement (Cc) allows the individualization
296 of the filled inner spaces of the fossilized bone (Fig. 4.6). The filling presents a geopetal
297 texture mainly in the cancellous bone spaces (external marrow portion), and the fractures
298 described above.

299 The same thin section observed without polarizing light (Fig. 4.2) shows empty
300 Canaliculi (C), Volkmann canals (Vc), and Haverssian canals (Hc) in the Ecb(Fig. 4.3),
301 whereas these structures are filled by Cc in the Icb and Tb (Fig. 4.5). The Cc presents in
302 two forms, as geopetal-coating with small crystals and with well-developed subhedral
303 sparite -type crystals, in the inner intertrabecular space. The Cc exhibits a centrifugal
304 growth, decreasing in abundance toward the external section (Gf in Fig. 4.6). Observations
305 of the sample with polarizing light, allow verification of the compounds and the presence of
306 empty spaces (isotropic components). The Cc presents two different textures. In the inner
307 walls of the spaces with trabecular tissue, crystals are tiny. However, crystals are large in
308 the central marrow cavity. Subhedral crystals have a centrifugal growth like those described
309 above (Fig. 4.6).

310

311 ***Scanning Electron Microscope (SEM)***

312 *Secondary Electrons*.- The light gray area (Fig. 5.1) corresponds to osteological
313 tissues. No empty spaces are observed, bone appears compact in section and the sub-
314 circular inner area is filled by mineral deposits, obliterating the marrow area of the
315 pneumatic bone. Periosteal bone is diagenetically altered (see the pitted margin), a fracture
316 with a clear filling of gypsum plates can be observed at the left (Fig. 5.2). This gypsum
317 grows fibrolamellarly between the bone and the inner fill in the medullar cavity.

318 *Backscattered electrons*.- Comparing the image observed with secondary electron
319 and backscattered electron modes in figures 5C and 5D respectively, two large well defined
320 areas can be distinguished regarding the atomic concentration in the sample (see Galván
321 Josa *et al*., 2013). The o light gray area represents the mineral fill in the medullar space
322 (Fig. 5.3). Dark gray portions correspond to compact bone, as well as to the fill obliterating
323 the inner spaces (marrow cavities), and the rest of the area corresponds to medullar bone
324 (lower part of the image, Fig. 5.4). Fractures appear in black color running along the
325 periosteal and compact layers, the little punctuated area representing the Haversian canals
326 (and the enlarged cavities), and diaclases. Brighter white dots correspond to indeterminate
327 minerals with a higher atomic density (Fig. 5.4).
328 *EDAX*.- The microanalysis of electrons (EDAX) made on the external portion of the
329 bone (see Fig. 5.5) in the same sample previously observed in SEM indicates the presence
330 of chemical elements mostly represented by calcium, phosphorus and oxygen characteristic
331 of the bone hydroxyapatite ($Ca_5(PO_4)_3OH$ or $Ca_{10}(PO_4)_6(OH)_2$). There is also a minor
332 proportion of sulfur, fluorine, and other subordinate complementary elements such as
333 carbon, silica, magnesium, sodium, and iron, in decreasing abundance (Fig. 5.5). At the
334 inner portion, phosphorus is scarce and fluor and sodium are totally absent (Fig. 5.6).
335 Among the complementary elements, magnesium is poorly represented, and iron disappears
336 and is substituted by manganese. They mostly correspond to the carbonate composition —
337 calcite $CaCO_3$/ dolomite $CaMg(CO_3)_2$ and manganocalcite $(CaMn)CO_3$— filling the inner
338 portion of the bone.
339
340 ***X-ray***

A complex series is formed by the varieties of Apatite in which the replacement of F^-, Cl^- and OH^- took place (Klein and Hurlbut, 1997). "Colofana" is the denomination of a dense and compact or cryptocrystalline variety of fluorapatite - $Ca_5(PO_4)_3F$ -present in fossil bones. It can take impurities or small quantities of calcium carbonate (Klein and Hurlbut, 1997) and combines as a solid solution with hydroxyapatite ($Ca_5(PO_4)_3OH$ or $Ca_{10}(PO_4)_6(OH)_2$) in biological matrices of original bones.

The following minerals appear in the diffractogram (mentioned in the prevalence order): fluorapatite "FAp" $Ca_5(PO_4)_3F$ and manganocalcite "MnCa" $(Ca,Mn)CO_3$, gypsum "Y" $CaSO_4\ 2H_2O$ (only in the Paleocene sample of *Crossvallia*), quartz "Q" SiO_2 and K-feldspar "FK" $KAlSi_3O_8$. A good crystallinity is observed in phosphates (Fig. 6.1), higher than that of the Antarctic fossil *Spheniscus* (Jadwiszczak *et al*., 2013b) and other minerals; mainly MnCa.

The diffractogram of the Eocene sample (Spheniscidae *indet*.) from Marambio (Seymour Island) shows a clear predominance of FAp and traces of Q. Cristallinity is similar to that one of *Crossvallia* (Fig. 6.2).

In the fresh bone of the living *Pygoscelis adeliae* collected at the same locality, appears a variety of apatite "Ap" $Ca_{10}(PO_4)_6(OH)_2$ usually hydroxyapatite (Montel *et al*., 1981), normally called "biogenic apatite or bioapatite", with a high content of organic matter. It is related to the poor crystallinity exhibited (Fig. 6.3).

DISCUSSION

The fossil record of the Cross Valley Formation was strongly constrained by biostratinomic and fossil diagenetic processes. They have left an easily recognizable imprint in the remains of *Crossvallia*, partially destroying other fossil evidence as well.

Apart from the plant remains preserved in the upper part of the C Allomember, a few fossil bones, shark and fish teeth, gastropods, bivalves and crinoids are the only body fossils preserved in this unit (see also Tambussi *et al*., 2005: p. 668).

The preliminary appraisal during macroscopic analysis indicates that holotype of *Crossvallia* was badly preserved; fossil bones appear in several pieces with altered surfaces (Tambussi *et al*., 2005). However, geochemical studies and microscopic analyses show the preservation of the composition and tissular structure, allowing further interpretations about preservation in this single bearing penguin level.

The lithological features of the Cross Valley C Allomember record a range of depositional settings from shallow marine to delta plain environments arranged in a shallowing upward trend. The erosional surface and the coarse-grained (breccia) deposits at the base of the upper allomember suggest an initial period of erosion and reworking of the underlying sediments. The fossiliferous gray mudstones with marine invertebrates point to a marine environment either below the wave base or protected from the wave action (like a coastal lagoon). The upper sandstones and mudstones lacking marine fossils but containing fossil wood, leaves and other plant debris suggest a deltaic environment. Overall C Allomember is thought to represent deposition during a transgressive-regressive cycle.

Taphonomy history

The taphonomic pathway of *Crossvallia* was interpreted taking into account the mode of life of penguins. Considering that *Crossvallia* was a diving bird, we divided the taphonomic processes following Lawrence (1968; see however Fernández-López, 1988 for a different criterion).

389 *Biostratinomy*.- Considering the spatial relationships among skeletal elements in the
390 field, *Crossvallia* represents a typically parautochthonous record (Fig. 2). Fossils were
391 found disarticulated but associated (according to Behrensmeyer, 1991). The association of
392 the skeletal elements in an area of approximately 1 m^2 (see Tambussi *et al.*, 2005) suggests
393 only minor transportation of the remains (Fig. 2). The apparent rapid burial, is suggested
394 also by the absence of signs of weathering and abrasion of the periosteal bone. By contrast,
395 the lack of representation of any other element of this skeleton can be explained by fossil
396 diagenetic destruction (see conclusions below).The accompanying fish remains were also
397 found isolated and are badly preserved as well.
398 The absence of longitudinal fractures, eyelet fractures, or periosteal bone damage in
399 *Crossvallia*, indicates that weathering did not affect bones before burial (between stages 0/1
400 of Behrensmeyer, 1978). Moreover, previous disarticulation followed by early burial are
401 also interpreted from the absence of irregular fractures produced when collagen was still a
402 constituting part of the bone like in modern skeletons (see example of fractures in penguin
403 bones in Acosta Hospitaleche *et al*., 2012).
404 *Fossil-diagenesis*.- The transversal or oblique disposition of the fractures described
405 above respect to the osteological tissue fibers, suggests that they had a fossil diagenetic
406 origin. Damage described in the tibiotarsal and femoral epiphyses, diaphysis filling,
407 corrosive deterioration of surfaces, mineral attachments (coating) of sulfates (gypsum), and
408 siliceous grains preserving the bone morphology after dissolution were a consequence of
409 geochemical processes occurred during burial and fossil diagenetic times. The dissolution
410 of surficial grains occurred by contact between elements of different chemical composition
411 (bioapatite of phosphatic bone and quartzose siliceous sediment) and produced a material
412 replacement keeping the original morphology.

413 Regarding the inner structure, there is no replacement of tissue composition. A
414 normal interference color in the petrographic sections indicates the preservation of the
415 original bioapatite composition. Carbonate cement fills the inner spaces as coating on the
416 walls and as crystals in the central area. A centrifugal growth of those fillings suggests that
417 solutions percolated through diagenetic fractures (Fig. 4.6). Sulphate deposits (gypsum-
418 anhydrite) observed in SEM images (Fig. 5.2) account for the acceleration of the
419 destruction of the remains due to their expansionary growing force. Gypsum was already
420 described as late cement formed during telogenesis in sandstones of the overlying La
421 Meseta Formation (Marenssi and Net, 1999). Breakage of clasts by growing of expansive
422 calcite cement was also described for the Cross Valley and Sobral sandstones (Marenssi *et*
423 *al*., 2012). In addition, the wedge action of ice, normal in the Antarctic seasonal dynamics,
424 might have promoted further destruction of the materials at or near the present-day surface.
425 It could also produce the initial fracture and crackled of bones, resulting in numerous little
426 and indeterminate bony fragments as the associated to the holotype mentioned above.
427 The fossil diagenesis in marine environments facilitates the replacement of OH^- by
428 F^- (Jadwiszczak *et al*., 2013b). That produced the changes in the apatite series as explained
429 above. In the particular case of *Crossvallia*, increasing substitution is given by fluorine
430 released by leaching of volcaniclastic sediments of the Cross Valley Formation. The
431 cristallinity of the Apatite indicated by sharp peaks in the Rx (Fig. 6.1) would be the
432 product of fossilization of the remains (see Jadwiszczak *et al*., 2013b). Consequently, it is
433 low in the fresh bone sample (see Fig. 6.3).
434 The manganocalcite filling of the inner spaces in *Crossvallia* would have
435 precipitated during burial. The fractures passing through the periosteal layer to the medullar
436 space were filled by gypsum, a late precipitate, probably near to the surface. The alternate

presence/absence of water would have produced the destruction of bones by successive expansion/contraction of gypsum. Differences in the atomic densities between bone and filling are evident through the backscattered electron mode (Fig. 5.4).

Palaeobiological considerations

Beyond the taphonomic scope of this paper, some interesting findings about the specimen under study deserve some comments. Firstly, the fossils analyzed belong to an undeniable diving bird, although the degree of specialization seems lower respect to other penguins, including fossil and modern species. It is particularly interesting because the pachyostosis (in this case, pachyosteosclerosis) is a non-pathological modification of the bone, directly related with the skills under water. It can be measured comparing the total thickness of the bone, which occupies 51% in *Crossvallia* (this paper), 55% in other Paleogene species such as *Palaeeudyptes*/*Anthropornis*, and 57% in the Neogene *Spheniscus uribinai* (Yury-Yañez *et al*., 2012). Results are consistent with the chronostratigraphical provenance of the compared remains, and the expected trend of specialization for diving.

Another interesting and unexpected result is the presence of large resorption cavities found in the cortical bone definitively related to molt cycles (Fig. 4.5). The compact bone undergoes a series of changes during the molt cycle, correlated with the increasing need for calcium. It involves the enlargement of the Haversian system producing cavities by erosion and resorption of the bone substance followed by a deposition of new bone and formation of a new Haversian system (Meister, 1951; Kuenzel, 2003).

The cavities and the accompanying secondary osteons point that MLP 00-I-1-16 was an adult penguin that experimented molts more than once. Consistent with this idea is

461 the thickness of the outer periosteal layer (Fig. 4.6) indicating that MLP 00-I-1-16 was a
462 mature bird.

463 Besides, and even when discussion about the medullary bone in reptiles is wide and
464 persistent (Schweitzer *et al*. 2007, Prondvai and Stein, 2014), there is consensus about its
465 meaning in birds (Meister 1951, Chinsamy *et al*., 2013). This tissue is only present in
466 reproductively active females. Several studies demonstrated that medullary bone is directly
467 related to the maturation of the ovarian follicles before egg laying, working as a calcium
468 reservoir for the production of the calcareous eggshell (Dacke *et al*., 1993). We interpret as
469 medullar bone the trabecular tissue invading the medullar space (Fig. 4.1, 4.5). It implies
470 that the specimen under study would have passed at least for one ovulating period before
471 death.

472

473 **CONCLUSIONS**

474 Given the evidence presented here, this specimen of *Crossvallia unienwillia* is
475 interpreted as an adult female that passed through several molting periods, which was
476 adapted to diving, although not so extremely adapted as the modern species. Fossil bones of
477 *Crossvallia* are associated with a typical marine assemblage including sharks and
478 macroinvertebrates in the *Cross Valley C Allomember* (former Bahía Pingüino Member,
479 Tambussi *et al*., 2005). The hosting mudstones point to a low-energy environment either
480 below the wave-base (prodelta) or protected from the wave action (lagoon or
481 interdistributary bay). In any case initial marine conditions changed to other with regular
482 influx of land-derived (woods and leaves) material (Marenssi *et al*., 2012).

483 The bounded spatial distribution and the preservational features described for
484 remains of *Crossvallia* suggest biostratinomic processes consistent with little transport and

485 rapid burial, which would have prevented the action of destructive processes, such as
486 weathering and predation. The rapid burial favored the initial preservation of the elements
487 under anoxic conditions. This is supported by the presence of manganocalcite observed in
488 the diffractogram (developed under anoxic conditions) and by the bone tissue structure, the
489 state of the epiphysis, and the preservation of the periosteal bone. The OH^- of the original
490 hydroxyapatite ($Ca_5(PO_4)3OH$) commonly known as bioapatite in the bones, was
491 substituted by F^- and preserved as fluoro-apatite ($Ca_5(PO_4)3F$), which provided a higher
492 resistance to destruction occasioned by chemical corrosion or mineral replacement.
493 The surficial corrosion, fractures, and the internal filling of the cavities, suggest that
494 destructive processes were only important after final burial during the telodiagenetic stage.
495 The absence of more vertebrate fossil remains, including other parts of the *Crossvallia*
496 skeleton, in the *Cross Valley C* Allomember could be the result of those processes, whereas
497 on the contrary, the original depositional environment appears to be optimal.
498
499 **ACKNOWLEDGEMENTS**
500 We thank to Dr. Daniel Poiré, for his collaboration in the X-ray analysis, Lic. Nadia
501 Haidr for her help with the paleohistology interpretation, the Consejo Nacional de
502 Investigaciones Científicas y Técnicas and the Agencia Nacional de Promoción Científica y
503 Tecnológica (PICT 2010 0093, PICT 2011 0284) for financial support. Instituto Antártico
504 Argentino provided logistic support in Antarctica. To the technical personnel of the LIMF
505 service (Facultad de Ingeniería, UNLP) and Laboratory of Diffraction of Rx and
506 petrography of the CIG-CONICET, for the analytic determination and the preparation of
507 the fossil material. To Lic. Daniel Cabrera for assistance with images obtained by binocular
508 microscope.

REFERENCES

Acosta Hospitaleche, C., Pérez, L., Acosta, W., and Reguero, M. 2012. A traumatic fracture in a giant Eocene penguin from Antarctica. *Antarctic Science* 24: 619-624.

Amoedo, P.E. 1992. **[***Estudio sedimentológico de la Formación Cross Valley, isla Marambio, Antártida*. Tesis Licenciatura, Facultad de Ciencias Exactas y Naturales, Universidad de Buenos Aires, Buenos Aires, 128 p. Unpublished]

Askin, R. 1988. Campanian to Paleocene palynological succession of Seymour and adjacent islands, northeastern Antarctic Peninsula. In: R.M. Feldmann, and M.O. Woodburne (Eds.), *Geology and Paleontology of Seymour Island, Antarctic Peninsula*. Geological Society of America, Memoir 169, p. 131–153.

Baumel, J., and Witmer, L. 1993. Osteología. In: J. Baumel, A. King, J. Breazile, H. Evans, and J. Vanden Berge (Eds.), *Handbook of Avian Anatomy. Nomina Anatomica Avium, second ed.* Publications of Nutall Ornithological Club, Cambridge, Massachussets, p. 45–132.

Behrensmeyer, A. K. 1978. Taphonomic and ecologic information from bone weathering. *Paleobiology* 4: 150–162.

Behrensmeyer, A.K., 1991. Terrestrial vertebrate accumulations. In, Allison, P.A., Briggs, D.E.G. (Eds.), Taphonomy, Releasing the data locked in the fossil record, Topics in Geobiology 9. Plenum Press, New York, pp. 291–335.

Cantrill, D.J., Tosolini, A-M.P., and Francis, J.E. 2011. Paleocene flora from SeymourIsland, Antarctica: revision of Dusén's (1908) pteridophyte and conifer taxa. *Alcheringa* 35: 309–328.

532 Cerda, I.A., Tambussi, C.P., and Degrange, F.J. 2015. Unexpected microanatomical
533 variation among Eocene Antarctic stem penguins (Aves: Sphenisciformes).
534 *Historical Biology* 27: 549–557.
535 Chinsamy, A., Chiappe, L., Marugán-Lobón, J., Chunling, G., and Fengjiao, Z. 2013.
536 Gender identification bird *Confuciosornis sanctus. Nature Communications* 4:
537 1381.
538 Cione, A., Acosta Hospitaleche, C., Pérez, L., César, I., and Laza, J. 2010. Fossil traces on
539 penguin bones from the Miocene of Southern Argentina. *Alcheringa* 34: 433–454.
540 Dacke, C.G., Arkle, S., Cook, D.J., Wormstone, I.M., Jones, S., Zaidi, M., and Bascal, Z.A.
541 1993. Medullary bone and avian calcium regulation. *Journal of Experimental*
542 *Biology* 184: 63–88.
543 de Margerie, E., de Robin, J.P., Verrier, D., Cubo, J., and Castanet, J. 2004. Assessing a
544 relationship between bone microstructure and growth rate: a fluorescent labelling
545 study in the king penguin chick (*Aptenodytes patagonicus*). *Journal of*
546 *Experimental Biology* 207: 869–879.
547 de Ricqlès, A, and de Buffrénil, V. 2001. Bone histology, heterochronies and the return of
548 the tetrapods to life in water. where are we?. In: J. Mazin, and V. de Buffre´nil
549 (Eds.), *Secondary adaptation of tetrapods to life in water.* Friedrich Pfeil,
550 Munchen, 367 p.
551 Doktor, M., Gazdzicki, A., Marenssi, S.A., Porebski, S.J., Santillana, S. N., and Vrba, A.V.
552 1988. Argentine-Polish geological investigations on Seymour (Marambio) Island,
553 Antarctica. *Polish Polar Research* 9: 521–541.

554 Dusén, P. 1908. Uber die tertiäre flora der Seymour-Insel. In: O. Nordenskjold (Ed.),
555 *Wissensschafttliche Ergebnisse der Schwedischen Südpolar Expedition 1901-103*.
556 Stockholm, 3 p. 1–27.
557 Elliot, D., and Trautman, T. 1982. Lower Tertiary strata on Seymour Island, Antarctic
558 peninsula. In: C. Craddock (Ed.), *Antarctic Geoscience*. University of Wisconsin
559 Press, Madison, p. 287–297.
560 Elliot, D.H., Rinaldi, C.A., Zinsmeister, W., Trautman, T.A., Bryant, W. A., and Del Valle,
561 R.A. 1975. Geological investigations on Seymour Island, Antarctic Peninsula.
562 *Antarctic Journal of the United States* 10: 182–186.
563
564 Fernández- López, S., 1988. Bioestratigrafia y Biocronología: su desarrollo histórico. Curso
565 de conferencias sobre Historia de la Paleontología (B. Meléndez, coordinador.
566 1987). Real Academia de Ciencias Exactas, Físicas y Naturales. Historia de la
567 Ciencia, Historia de la Paleontología: 185–215.
568 Galván Josa, V., Fracchia, D., Castellano, G., Crespo, E., Kang, A., and Bonetto, R. 2013.
569 Backscattered electron images, X-ray maps and Monte Carlo simulations applied to
570 the study of plagioclase composition in volcanic rocks. *Spectrochimica Acta Part B*
571 81: 50–58.
572 Hombron, J.B. y Jacquinot, H. 1841. Description de plusieurs oiseaux nouveaux ou peu
573 connus,provenant de l'expédition autour du monde faite sur les corvettes 'l'Astrolabe
574 et la Zelée. *Annales Des Sciences Naturelles, Zoologie* 16: 312–320.
575 Houssaye, A. 2009. “Pachyostosis” in aquatic amniotes: a review. *Integrative Zoology* 4:
576 325–340.

577 Jadwiszczak, P., Acosta Hospitaleche, C., and Reguero, M. 2013a. Redescription of
578 *Crossvallia unienwillia*: the only Paleocene Antartic Penguin. *Ameghiniana* 50:
579 545–553.
580 Jadwiszczak, P., Krajewski, K.P., Pushina, Z., Tatur, A., and Zieliński, G. 2013b. The first
581 record of fossil penguins from East Antarctica. *Antarctic Science* 25: 397– 408.
582 Klein, C., and Hurlbut, C.S. Jr. 1997. *Manual de Mineralogía (Basado en la obra de J. D.*
583 *Dana)*. Cuarta Edición, Vol 2. Reverté, Barcelona. 679 p.
584 Kuenzel, W.J. 2003. Neurobiology of Molt in Avian Species. *Poultry Science* 82: 981–991
585 Lawrence, D.R. 1968. Taphonomy and information looses in fossil communities. Geological
586 Society of American Bulletin 79: 1315–1330.
587 Marenssi, S.A., and Net, L.I. 1999. Presencia de yeso diagenético como cemento en las
588 areniscas de la Formación La Meseta, isla Marambio, Antártida. *IV Jornadas sobre*
589 *Investigaciones Antárticas*. Buenos Aires, Actas 2: 348–351.
590 Marenssi, S.A., and Santillana, S.N. 2003. $^{87}Sr/^{86}Sr$ derived ages from the lower Sobral
591 Formation, Paleocene, Seymour Island, Antarctica Peninsula. *IX ISAES, Potsdam*.
592 Programme and Abstracts, 219–220.
593 Marenssi, S.A., Santillana, S.N., and Bauer, M. 2012. Estratigrafía, petrografía sedimentaria
594 y procedencia de las formaciones Sobral y Cross Valley (Paleoceno), Isla Marambio
595 (Seymour), Antártica. *Andean Geology* 39: 67–91.
596 Meister, W. 1951. Changes in histological structure of the long bones of birds during the
597 molt. *The Anatomical Record* 111: 1–21.
598 Meister, W. 1962. Histological structure of the long bone of penguins. *The Anatomical*
599 *Record* 143: 377–387.

600 Montel G., Bonel, G., Heughebaert, J.C., Trombe, J.C. and Rey C. 1981. New concepts in
601 the composition, crystallization and growth of the mineral component of calcified
602 tissues. *Journal of Crystal Growth* 53: 74–99.
603 Montes, M., Santillana, S.N., and Marenssi, S.A. 2007. Secuencias de relleno del valle
604 incidido en la Formación Cross Valley. Paleoceno superior de la isla Marambio
605 (Mar de Weddell, Antártica). *Simposio Argentino, No. 6 y Latinoamericano sobre*
606 *Investigaciones Antárticas, No. 3.* GEORE830: 4 pp. CD-ROM. Buenos Aires.
607 Montes, M., Nozal, F., Santillana, S.N., Marenssi, S.A., and Olivero, E. 2013. Mapa
608 geológico de la Isla Marambio (Seymour), Antártica; Escala 1:20000. 1ª edición.
609 Serie Cartográfica Geocientífica Antártica Geológico y Minero de España, Buenos
610 Aires. Instituto Antártico Argentino.
611 Palamarczuk, S., Ambrosini, G., Villar, H., Medina, F.A. Martinez Macchiavello, J.C., and
612 Rinaldi, C.A. 1984. Las Formaciones López de Bertodano y Sobral en la isla
613 Vicecomodoro Marambio, Antártida. *IX Congreso Geológico Argentino.* Bariloche.
614 *Actas* 1:7–24.
615 Prondvai, E., and Stein, K. 2014. Medullary bone-like tissue in the mandibular symphyses of
616 a pterosaur suggests non-reproductive significance. *Scientific Reports* 4: 6253
617 Sadler, P.M. 1988. Geometry and stratification of uppermost Cretaceous and Paleogene units
618 on Seymour Island, northern Antarctic Peninsula. In: R.M. Feldman, and M.O.
619 Woodburne (Eds.), *Geology and Paleontology of Seymour Island, Antarctic*
620 *Peninsula.* Geological Society of America, Boulder, Memoir 169, p. 303–320.
621 Santillana, S.N., and Marenssi, S. 1997. Descripción e interpretación de las discordancias
622 paleocenas de la isla Marambio, Antártica. *Jornadas sobre Investigaciones*
623 *Antárticas*, Buenos Aires, *Actas*: 262–266.

624 Santillana, S.N., Montes, M., and Marenssi, S. 2007. Secuencias Estratigráficas de la
625 Formacion Sobral, Paleoceno de la Isla Marambio (Mar de Weddell, Antártica).
626 *Simposio Argentino, No. 6 y Latinoamericano sobre Investigaciones Antárticas, No.*
627 *3*. GEORE829: 4 pp.CD-ROM. Buenos Aires.
628 Schweitzer, M.H., Elsey, R.M., Dacke, C.G., Horner, J.R., and Lamm, E.T. 2007. Do egg-
629 laying crocodilian (*Alligator mississippiensis*) archosaurs form medullary bone?.
630 *Bone* 40: 1152–1158.
631 Tambussi, C.P., Reguero, M.A., Marenssi, S.A., and Santillana, S.N. 2005. *Crossvallia*
632 *unienwillia*, a new Spheniscidae (Sphenisciformes, Aves) from the Late Paleocene
633 of Antarctica. *Geobios* 38: 667–675.
634 Wrenn, J.H., and Hart, G.F. 1988. Paleogene dinoflagellates cyst biostratigraphy of Seymour
635 Island. In: R. M. Feldmann, and M. O. Woodburne (Eds.), *Geology and*
636 *Paleontology of Seymour Island, Antarctic Peninsula.* Geological Society of
637 America, Boulder, Memoir 169, p. 321–447.
638 Yury–Yáñez, R.E., Ossa, L., Rubilar–Rogers, D., and Sallaberry, M. 2012. Inferring growth
639 in giant Penguins from the Paleogene of Antarctica and the Neogene of South
640 America. *Supplement to the online Journal of Vertebrate Paleontology*, 199.
641

642 **Figure captions**

643

644 **Figure 1. 1**, Map of the study area, the star points the ***Crossvallia*** locality; **2**, General
645 location of the Marambio (Seymour) Island indicated by the arrow; **3**, Stratigrahic scheme
646 showing the relationship of the Cross Valley Formation (modified from Montes *et al*.,
647 2013).

648

649 **Figure 2.** Image of the discovery with the specimen of ***Crossvallia unienwillia*** lying *in*
650 *situ*, where the space relationships among the penguin fossil bones are observed.

651

652 **Figure 3. 1**, Left humerus with oblique and transversal fractures in cranial view, see the
653 arrows; **2**, Right femur in cranial view (see the evidence of chemical corrosion in the
654 proximal epiphysis, and the transverse fractures in the distal end); **3**, distal epiphysis of
655 right tibiotarsus with signs of corrosion and mineral deposits. Scale bars: 50 mm.

656

657 **Figure 4.** Transversal sections in a diaphysis *of* ***Crossvallia unienwillia***. **1**, Relationship
658 between medullar spaces and the different layers of bone; **2**, Detail of the proportions
659 between the bone layers (Pb, Ecb, Icb and Tb), F1 running through the Pb and Icb, F2
660 running horizontally between the Pb and Ecb; **3**, compact periosteal bone and detail of the
661 Ft with fractures; **4**, compact bone and detail of the fibers organization; **5**, Icb with empty
662 and very developed Vc, Hc, see the C density, Tb with spaces filled by Cc, the arrows
663 signes the growing direction of carbonatic cement (Cc); **6**, secondary osteons surrounded
664 by lamellar tissue and carbonate minerals with Gf, the amorphous compound in the large
665 cavities originated by resorption, characteristic of the molt cycles. Image (1) was taken with

a binocular microscope, (2-6) were taken with a petrographic microscope; (4 and 6) taken with plane-polarizer (pp) and (2, 3, 5) without plane-polarizer (wp); Pb – periosteal bone; Ecb – external compact bone; Icb – inner compact bone; Tb – trabecular bone; Mc – marrow cavity; C – canaliculi; Po – primary osteons; So – secondary osteons; F1 – fracture 1; F2 – fracture 2; F3 – fracture 3; Ft – fibrollamelar tissue; Am – amorphous mineral; Hc – Haversian canals; Vc – Volkmann canals; Cc – carbonatic cement; Gf – geopetal filled. Scale bars: 20 mm (1), 100 μm (3), 200 μm (2, 3, 5, 6).

Figure 5. 1, Transversal sections of a long bone under SEM. Marrow cavity (Mc) fill and a large fracture with a mineral of laminar growth inside; **2**, Detail of the same image taken with Secondary Electrons. The light gray area corresponds to the compact bone (Cb), the dark gray central cylinder is the fill of the medullary space, the gypsum plate (G) is into the fracture. The arrows indicate the pitted margin in the external surface of the bone; **3**, Thin section of long bone with secondary electrons. External sector of bony fabric and small "islands" in the medullar space rounded by a mineral matrix; **4**, The same image done with backscattered electron mode, variations in tonality represent each different material. Light gray region is bone, whereas the dark gray represents the fill of medullar space (fractures and holes are in black); **5**, EDAX analysis of the external sector of the thin section, phosphorus corresponds to the chemical composition of the bone (see the arrow); **6**, EDAX analysis of the internal sector of the thin section, phosphorus disappears and Manganese belonging to the carbonate fill increases (see the arrow). Cb – compact bone; G – gypsum. Scale bars: 5 mm (1), 3 mm (2), 2 mm (3, 4).

689 **Figure 6.** Comparison of Rx diffractograms of selected penguin bones; **1**, Paleocene
690 ***Crossvallia unienwillia*** (see the fluorapatite with a good crystallinity); **2**, Eocene
691 Spheniscidae indet., (see the fluorapatite also with a good crystallinity but without
692 accessory minerals); **3**, The extant ***Pygoscelis adeliae*** (see the bioapatite with a low
693 crystallinity).

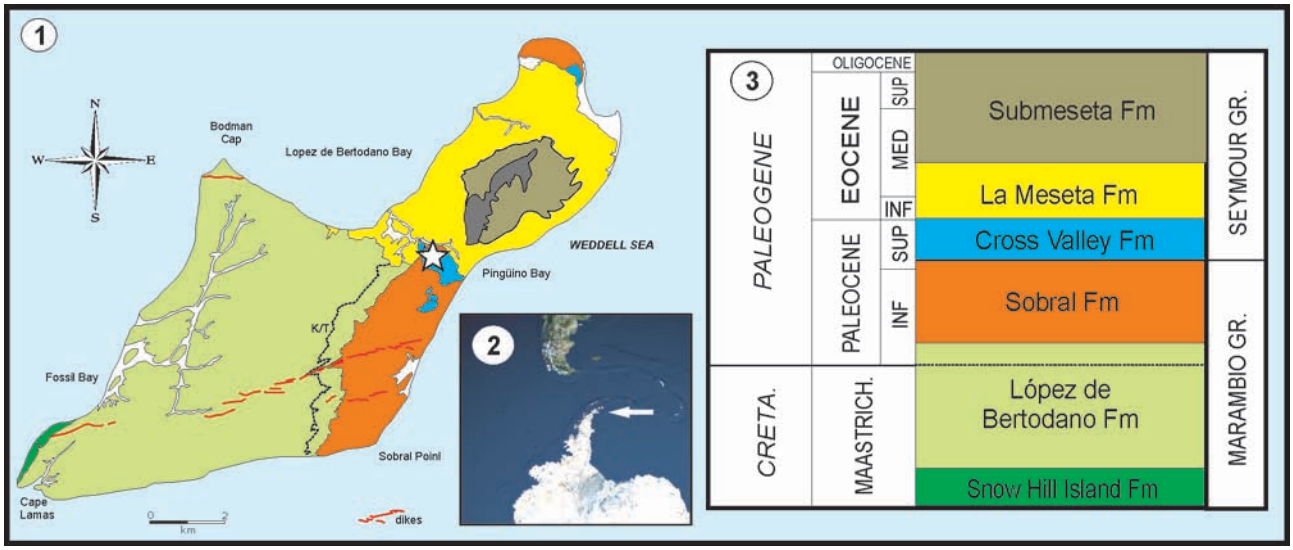
1
N
W
E
S
Bodman Cap
Lopez de Bertodano Bay
WEDDELL SEA
Pingüino Bay
K/T
Fossil Bay
Sobral Point
Cape Lamas
0
2
km
dikes
2
3
PALEOGENE
CRETA.
OLIGOCENE
EOCENE
PALEOCENE
MAASTRICH.
SUP
MED
INF
SUP
INF
Submeseta Fm
La Meseta Fm
Cross Valley Fm
Sobral Fm
López de Bertodano Fm
Snow Hill Island Fm
SEYMOUR GR.
MARAMBIO GR.

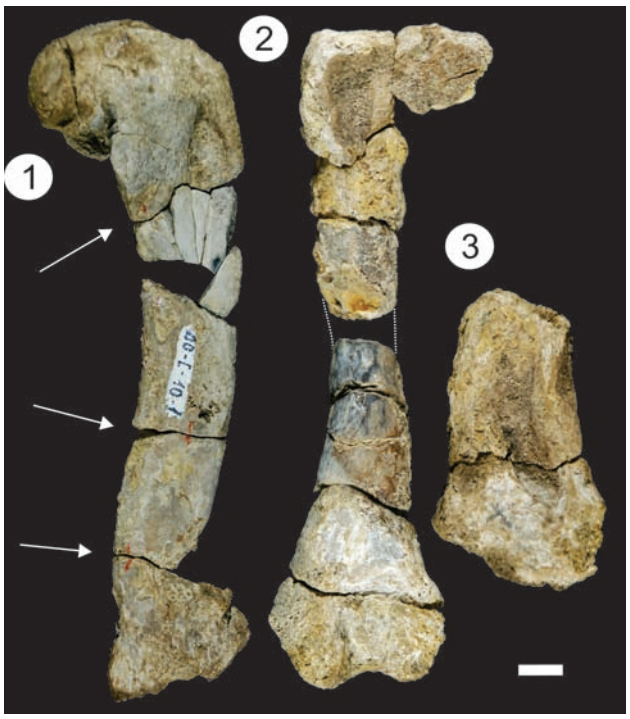
1
2
3

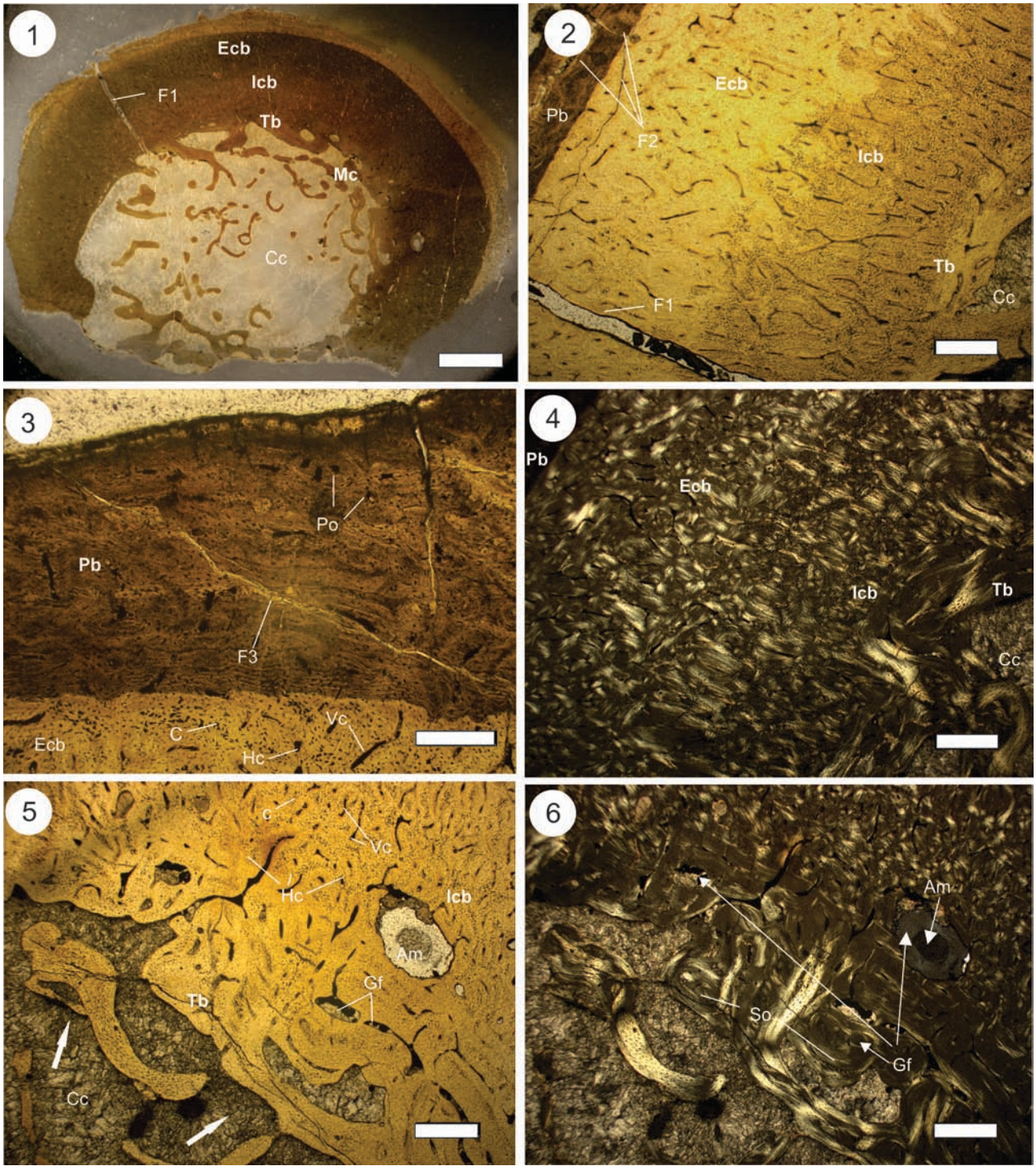
1
Ecb
Icb
F1
Tb
Mc
Cc
2
Ecb
Pb
F2
Icb
Tb
Cc
F1
3
Po
Pb
F3
Ecb
C
Vc
Hc
4
Pb
Ecb
Icb
Tb
Cc
5
c
Vc
Hc
Icb
Am
Gf
Tb
Cc
6
Am
So
Gf

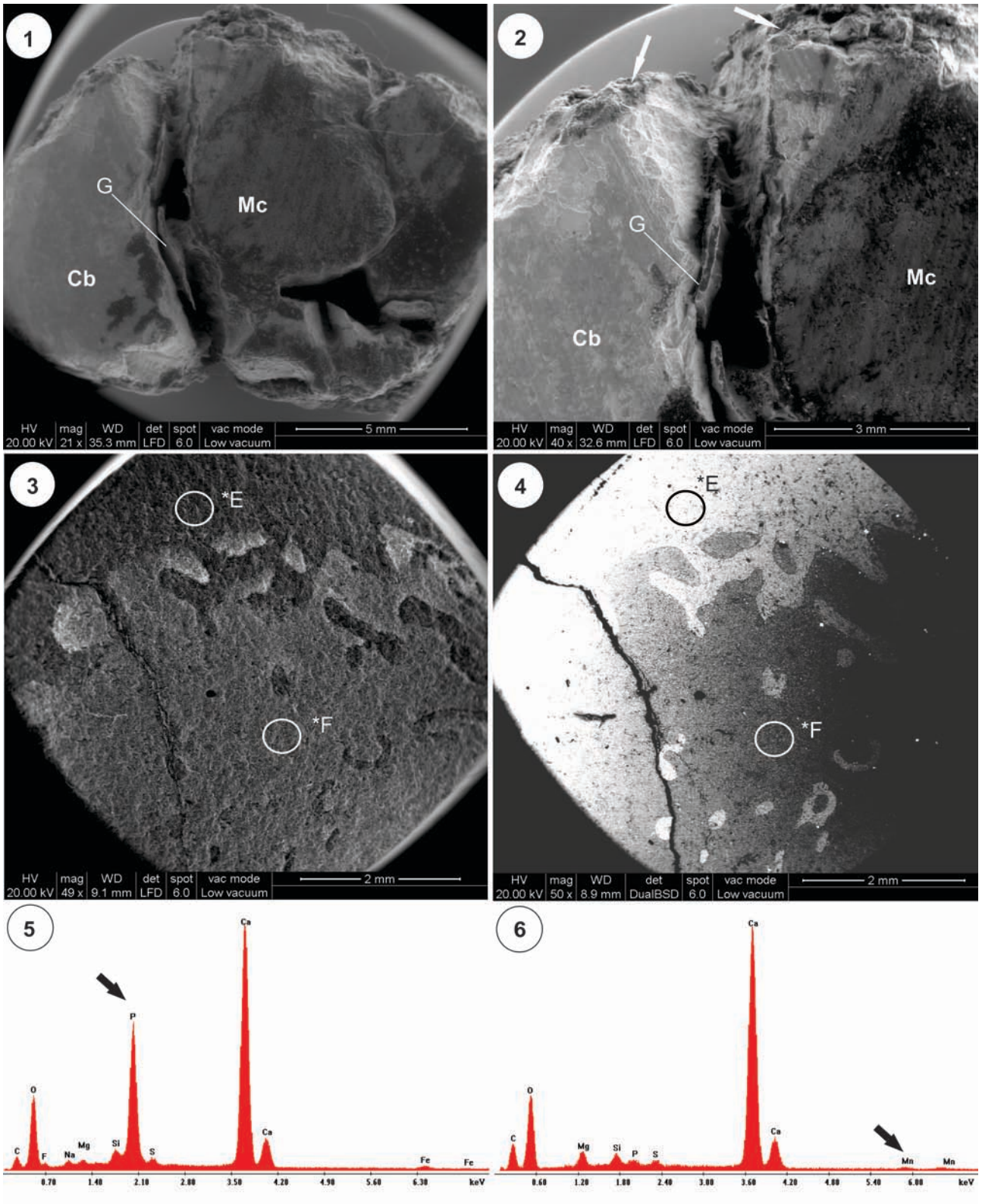
1
G
Mc
Cb
HV 20.00 kV | mag 21 x | WD 35.3 mm | det LFD | spot 6.0 | vac mode Low vacuum | 5 mm
2
G
Mc
Cb
HV 20.00 kV | mag 40 x | WD 32.6 mm | det LFD | spot 6.0 | vac mode Low vacuum | 3 mm
3
*E
*F
HV 20.00 kV | mag 49 x | WD 9.1 mm | det LFD | spot 6.0 | vac mode Low vacuum | 2 mm
4
*E
*F
HV 20.00 kV | mag 50 x | WD 8.9 mm | det DualBSD | spot 6.0 | vac mode Low vacuum | 2 mm
5
C O F Na Mg Si P S Ca Ca Fe Fe
0.70 1.40 2.10 2.80 3.50 4.20 4.90 5.60 6.30 keV
6
C O Mg Si P S Ca Ca Mn Mn
0.60 1.20 1.80 2.40 3.00 3.60 4.20 4.80 5.40 6.00 keV

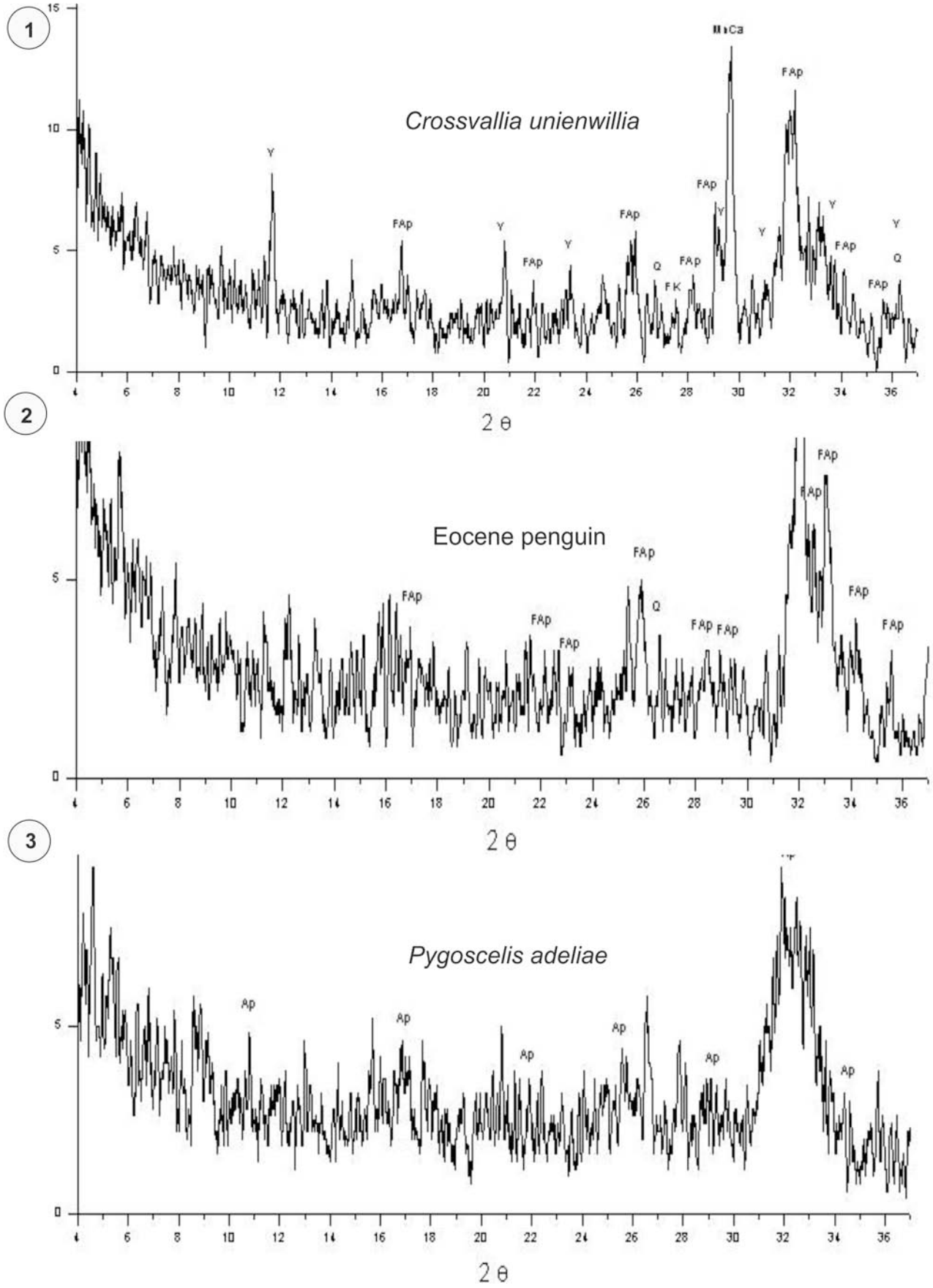
1
Crossvallia unienwillia
Y
FAp
Q
FK
MgCa
2 θ
2
Eocene penguin
FAp
Q
2 θ
3
Pygoscelis adeliae
Ap
2 θ